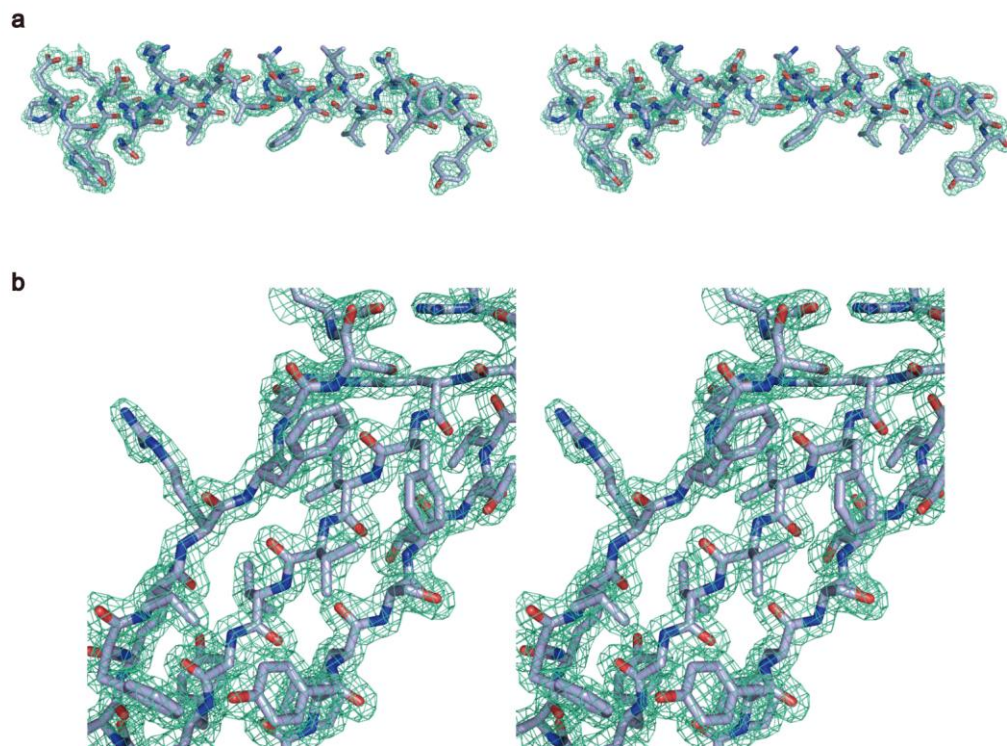


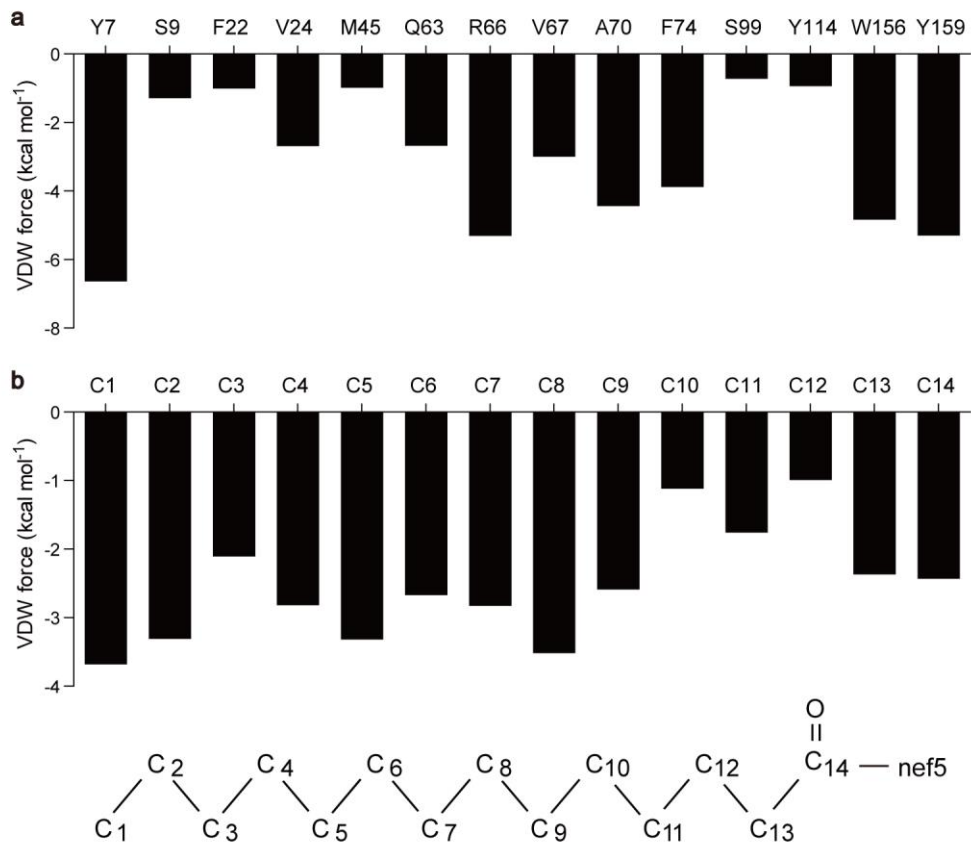
**Supplementary Figure 1. Involvement of an MHC class I molecule in lipopeptide Ag-presentation.**

**a**, 2N5.1 cells responded to C14nef5 to produce IFN- $\gamma$  in the presence of rhesus PBMCs derived from a positive donor, and the Ag-specific response was blocked by MB217 and MB226 mAbs (at a 1:400 dilution of ascites). **b**, Surface biotinylated LLC-MK2 cells were lysed in 0.5% Triton X-100, and immunoprecipitation was performed with the indicated mAbs. The 45 kDa species (MHC class I heavy chains) and 12 kDa species ( $\beta$ 2m) immunoprecipitated by the Abs were indicated. **c**, MB217 failed to recognize the human monocytic cell line, THP-1, but reacted to rhesus  $\beta$ 2m-transfected THP-1 cells (upper panels). MB226 failed to recognize the human  $\beta$ 2m-deficient cell line, FO-1, but reacted to human  $\beta$ 2m-reconstituted FO-1 cells (lower panels), indicating that MB226 cross-reacted to human

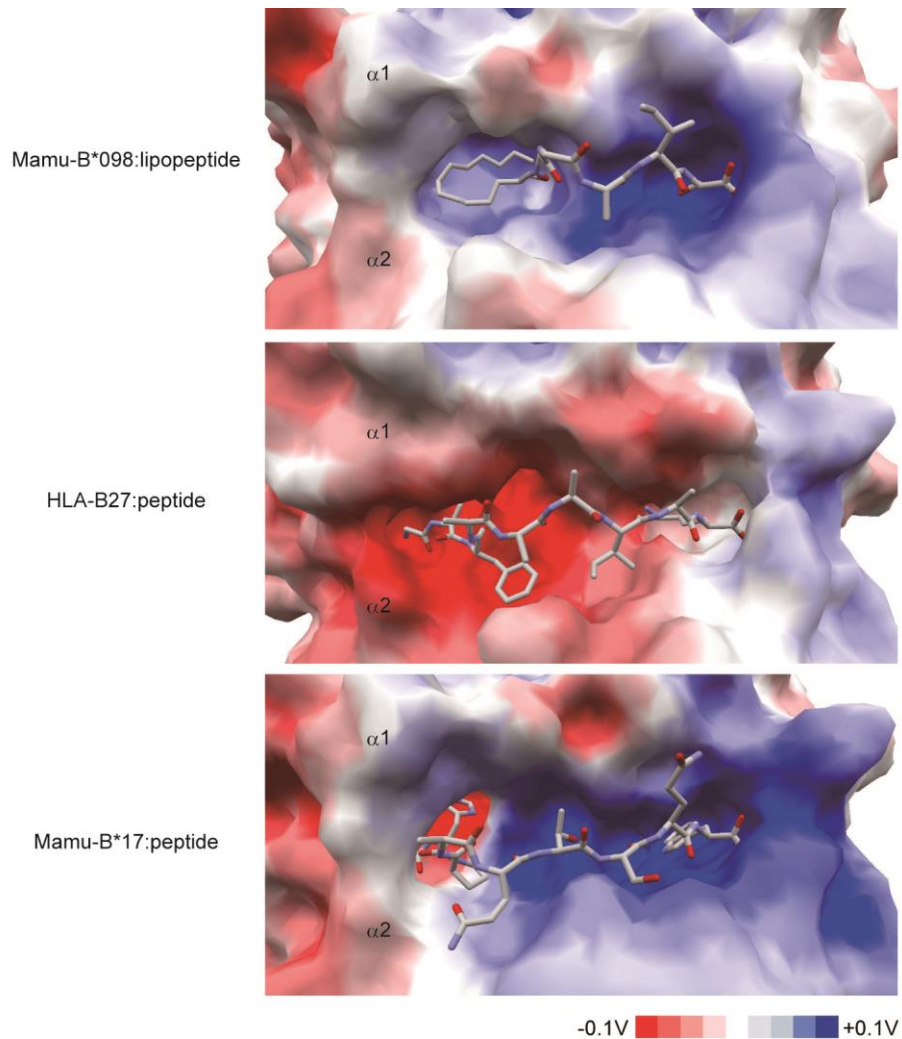
MHC class I molecules. Dotted lines indicate histograms with a negative control mAb. **d**, The mouse melanoma cell line, B16F10, was transfected transiently with the indicated genes, labeled with the MB226 mAb, and analyzed by flow cytometry. **e**, The reactivity of serially diluted MB217 ascites to plate-coated human (left) and rhesus (right)  $\beta$ 2m was tested by ELISA. The reciprocal recognition of human and rhesus  $\beta$ 2m by BBM.1 and MB217 was demonstrated. Experiments were performed in triplicate, and mean values with SEM are shown.



**Supplementary Figure 2. Stereo images of a portion of the electron density map.** Stereo views of  $\alpha 1$  helix from Pro75 to Tyr85 (a) and  $\beta$ -sheets from Gly1 to Asp39 (b) of Mamu-B\*098 with a 2Fo-Fc map (green mesh) contoured at  $1.6\sigma$ .



**Supplementary Figure 3. VDW forces established between Mamu-B\*098 and the acyl chain of C14nef5.** The VDW forces involved in accommodation of the acyl chain were calculated for each amino acid residue of Mamu-B\*098 (**a**) and for individual carbons of the acyl chain (**b**) by a fragment molecular orbital (FMO) method using the PAICS program. Only the amino acid residues of Mamu-B\*098 with delta energy below the level of -0.5 kcal/mol are shown in **a**.



**Supplementary Figure 4. Surface electrostatic potential of Mamu-B\*098, HLA-B27, and Mamu-B\*17.** Surface electrostatic potentials of the Ag-binding groove are shown for Mamu-B\*098, HLA-B27, and Mamu-B\*17. Note the low electrostatic potential in the area involved in interactions with the acyl chain (top), which contrasted sharply with the high electrostatic potential detected in HLA-B27 (middle) and Mamu-B\*17 (bottom).



**Supplementary Table 1.** Contacts between C14nef5 and Mamu-B\*098

C14nef5	Hydrogen bonds			C-C contacts
	Atom	Partner	Distance (Å)	
Myristoyl group	O1	Y114 (OH)	3.1	Y7, S9, F22, V24, Q63, R66, V67, A70, F74, W156, Y159, 10 intrachain interactions
Gly1	O	Water384	3.1	None
		D69 (OD2)	2.9	
Gly2	O	T73 (OG1)	2.7	T73
		None		
Ala3	O	Water139	3.0	T73, W147, V152
		Water384	3.3	
Ile4	O	W147 (NE1)	2.9	T73, V76, S 77, N80
Ser5	N	S77 (OG)	3.0	S77, L81, Y84, T143, K146, W147
		OG	Q116 (OE1)	
	O	Water139	2.8	
		Y84 (OH)	2.7	
		T143 (OG1)	2.7	
	OXT	N80 (ND2)	2.9	
		Y84 (OH)	3.3	
		K146 (NZ)	2.9	

\* Contacts were assigned using a cut-off of 3.4 Å for hydrogen bond interactions and 4.4 Å for C-C interactions.